Soliton interaction and stability in nonlinear directional fiber couplers

Gil Cohen
Racah Institute of Physics, Hebrew University of Jerusalem, Jerusalem 91904, Israel
(Received 12 April 1995; revised manuscript received 21 June 1995)

The interaction of soliton pulses in the optical-fiber nonlinear directional coupler is studied theoretically and numerically. Using the Hamiltonian structure of the equations, a canonical perturbation theory is developed and the steady-state regimes of the two-soliton system are found. Linear stability analysis shows that, in general, none of these states are stable. Numerical simulations performed support, both qualitatively and quantitatively, the theoretical predictions.

PACS number(s): 42.81.−i, 42.50.Ne

I. INTRODUCTION

Optical solitons in fiber waveguides are considered as the future bits of very high speed digital data communication systems. This is due to their unique property [1] of propagation without dispersion or distortion, over very long distances [2]. In order to exploit the high data transmission rates of solitons in fibers, all optical-fiber components, which will be able to control and manipulate the soliton bits, must be found. One of the most promising candidates for the "optical switch" is the nonlinear directional coupler (NLDC) [3,4]. The switching properties of this device have been studied experimentally [5,6] and theoretically [7–10]. Soliton pulse switching was described in the framework of a variational approach [11] in [7] and in [8] (in [8] a more complete trial function was employed). Switching of soliton pulses was investigated numerically in [9]. In [10], a variant of the variational method was applied to Gaussian shaped pulses. Another potential application of the NLDC is to use it as a building block for all digital soliton bit processing. For this purpose, one must investigate the behavior of solitons interacting in the NLDC.

The evolution of envelope pulses in single-mode optical-fibers can be described by the nonlinear Schrödinger equation (NLSE) [12]. The NLSE is integrable by the inverse scattering method [13] and stable solitons are (some of) its solutions. Soliton interaction in the NLDC is described by two coupled NLSE's [see Eqs. (1), Sec. II]. Generally, coupled NLSE's are not completely integrable [14]. In this situation, one can think of two alternative directions of investigating pulse propagation phenomena in the NLDC. In the first, one looks for soliton states of the NLDC that do not exist as stable solutions of the single NLSE. This approach is applicable regardless of the strength of the coupling between the fibers and is especially suitable when the coupling is strong. In [15], it was found that there exist symmetric and asymmetric stationary coupled soliton states of the NLDC. Bifurcations from both solutions to functionally different, asymmetric states were identified, analytically for the symmetric state and numerically for the asymmetric state [15]. A linear stability analysis of all these state was carried out in [16,17], where it was shown that the symmetric state becomes unstable after the bifurcation of the new asymmetric state, which by itself is stable. For the asymmetric branch, it was found that it loses its stability before the bifurcation point and that the branching asymmetric solution is also unstable [16,17]. The second direction addresses the soliton pulses that exist in the single NLSE and deals with their interaction in the NLDC. This approach is especially relevant when the coupling between the two adjoining fibers is weak, since it is then natural to assume that it would act as a perturbation to the single-fiber soliton states.

In this (second) case one would then want to study the soliton states of the single NLSE that the NLDC can support, and their stability, by means of perturbation methods. In previous works using perturbation methods, initial soliton pulse profiles with a limited range of parameter values were considered [7,18,19]. Also, only limited types of perturbations to these profiles [7,18–21] were investigated.

In this work we consider the general one-soliton pulse that can persist in an unperturbed single-mode fiber and look at the evolution of *all* its parameters during the interaction, with a similar pulse in the adjoining fiber, in the NLDC. We shall investigate the situation in which the initial conditions are in the form of one-soliton solutions in *both* the fibers. We shall be interested in the evolution of both these pulses under the influence of the neighboring pulse in the adjoining fiber. Using the Hamiltonian structure of the equations for the evolution of pulses in the NLDC, we shall be able to look at the evolution of all the soliton parameters during their interaction in the NLDC. By doing so, we can find the bound states of the (initial) solitons in the fibers and investigate their stability. This would help us to look at the possibilities of using the NLDC as a soliton processing logical element.

The paper is organized as follows. Section II presents the equations for the evolution of envelope pulses in the NLDC. In Sec. III the Hamiltonian formalism for the coupled NLSE's is outlined and the reduced equations are canonically transformed (using the integrals of motion of the system) to new coordinates. Section IV deals with the steady-state points of the reduced Hamiltonian system. The linear stability of the steady-state points is investigated in Sec. V. Numerical simulations that verify

the analytical results are presented in Sec. VI. Section VII summarizes our results. In the Appendix a detailed derivation of the steady-state points is carried out.

II. COUPLED NLSE'S

The equations for the envelope of pulses, centered around frequency ω_0, in two adjoining single-mode fibers interacting in the NLDC are [9]

$$i\frac{\partial\psi_1}{\partial x}+\frac{\partial^2\psi_1}{\partial t^2}+2\left|\psi_1\right|^2\psi_1+\alpha\psi_2=0, \tag{1a}$$

$$i\frac{\partial\psi_2}{\partial x}+\frac{\partial^2\psi_2}{\partial t^2}+2\left|\psi_2\right|^2\psi_2+\alpha\psi_1=0, \tag{1b}$$

where we have written the equations in soliton [22] units. x is the normalized (to the dispersion length) distance of propagation along the fiber axis; t is the normalized (to the pulse duration) time, in a frame of reference moving with the group velocity; $\psi_i\,(i=1,2)$ are the scaled amplitudes. α is the (dimensionless) coupling coefficient between the pulses in the fibers and is assumed to be small. This can be achieved, even for soliton pulses for which the dispersion length is large, due to the exponential fall of α with the distance between the adjoining fibers [23].

In writing the interaction of pulses in the NLDC in the form of Eqs. (1), we assume that the pulses in both fibers have the same group velocity and the same dispersion coefficient. That is, they correspond to envelopes of pulses centered around the same frequency ω_0. When this is the case, α can be chosen to be real. The interaction term arises from the overlapping of the evanescent field of the transverse fiber mode with the field in the adjoining fiber core [23]. It is assumed that the transverse fiber mode is not affected by the proximity of the adjoining fiber and by the existence of an identical transverse mode in it. We also assume that the interaction term arising from the cross phase modulation (terms proportional to $\left|\psi_i\right|^2\psi_{3-i}, i=1,2$) can be neglected.

The unperturbed ($\alpha=0$) equations are integrable [13] and their solutions consist of solitons and radiation. The one soliton solution is given by

$$\psi\left(t,x\right)=\frac{\frac{\rho}{2}\exp\left\{i\left(\frac{pt}{2}+\frac{\left(\rho^2-p^2\right)x}{4}-\varphi-\frac{\pi}{2}\right)\right\}}{\cosh\left\{\frac{\rho}{2}\left(t-px-\frac{2q}{\rho}\right)\right\}} \tag{2}$$

where ρ, p, q, and φ are free parameters of this solution. ρ defines the amplitude *and* width $(1/\rho)$ of the soliton, p is the soliton's velocity, $2q/\rho$ is its "center of mass," and φ is its "initial" phase.

III. HAMILTONIAN FORMALISM

Equations (1) can be derived from the Hamiltonian

$$H=\int_{-\infty}^{\infty}\left(\left|\frac{\partial\psi_1}{\partial t}\right|^2+\left|\frac{\partial\psi_2}{\partial t}\right|^2-\left|\psi_1\right|^4-\left|\psi_2\right|^4-\alpha 2\mathrm{Re}\left(\bar{\psi}_1\psi_2\right)\right)dt, \tag{3}$$

with

$$\frac{\partial\psi_i}{\partial x}=-i\frac{\delta H}{\delta\bar{\psi}_i}, \tag{4}$$

where $\bar{\psi}_i$ is the complex conjugate of ψ_i. After transforming from q to $q-\frac{\rho px}{2}$ and from φ to $\varphi-\frac{\left(\rho^2-p^2\right)x}{4}$, the parameters of the single-soliton solution [Eq. (2)] can be viewed [24] as a Hamiltonian system with ρ and φ, p and q canonically conjugate. The (reduced) one-soliton Hamiltonian is given by

$$H=\frac{1}{4}\left(\rho p^2-\frac{1}{3}\rho^3\right). \tag{5}$$

In view of this Hamiltonian formalism, we apply the following ansatz. We shall treat the perturbed system as a Hamiltonian system of "coupled" single solitons. The phase space of this Hamiltonian system is the solitons's parameter space, which is eight-dimensional. Assuming this, we may only investigate the evolution of the parameters of a single-soliton under the influence of another single-soliton in the adjoining fiber. We are thus neglecting radiation effects and the possible formation of other solitons. The physical motivation and justification for these assumptions is that we want to investigate the behavior and interaction of soliton pulses in optical fibers. Therefore, our initial condition, for each of the two fibers, will always be of the type of a single-soliton solution of the unperturbed NLSE. Also, it is known that solitons are robust objects. Therefore, since we are assuming that the coupling is small, it is meaningful to assume that the main effect will be that of the solitons persisting, but changing their shape and velocity by means of the evolution of their parameters. Note that the dimensionless form in which Eqs. (1) are written implies that, for solutions of the form of Eq. (2), the contribution of the nonlinear term will be substantial provided that $\rho\gtrsim 1$. Since we are assuming that $\alpha\ll 1$, we obtain that, within the framework of our ansatz, $\rho\gg\alpha$.

The reduced Hamiltonian of the perturbed system Eqs. (1) is

$$H=H_0+H_{\mathrm{int}}, \tag{6}$$

where

$$H_0=\sum_{i=1,2}\frac{1}{4}\left(\rho_i p_i^2-\frac{1}{3}\rho_i^3\right) \tag{7a}$$

and

$$H_{\mathrm{int}}=-\alpha\mathrm{Re}\left[\frac{\rho_1\rho_2}{2}\exp\left[i\left(\varphi_2-\varphi_1\right)\right]\times\int_{-\infty}^{\infty}\frac{\exp\left[i\left(p_1-p_2\right)\frac{t}{2}\right]}{\cosh\left(\frac{\rho_1 t}{2}-q_1\right)\cosh\left(\frac{\rho_2 t}{2}-q_2\right)}dt\right]. \tag{7b}$$

The Hamiltonian (6) describes a dynamical system, where x plays the role of "time." The subscripts 1 and 2 relate to the parameters of the first and second fiber, respectively. The unperturbed part, Eq. (7a), describes the evolution of the parameters of the single-soliton solution

in the fibers, not taking into account the influence of the pulse in the adjoining fiber. The interaction term, Eq. (7b), represents the effect that the presence of a pulse in the adjoining fiber has on the evolution of the parameters of the solitons. It is in fact an "overlap integral" (in time) of the pulses in the two fibers, for fixed distance of propagation x. For this integral to have a meaningful contribution to the Hamiltonian (6), the two solitons must be peaked around times that differ by less than the solitons' widths $1/\rho_i$. Also, the difference between the velocities of the solitons must not be too large (relative to ρ_i), so that the oscillatory term in the integral will not average out the interaction.

The perturbed system still has two conserved integrals (in contrast to the infinite number of conserved integrals of the unperturbed, integrable, system). The first one is

$$\int_{-\infty}^{\infty}\left(|\psi_1|^2+|\psi_2|^2\right)dt, \tag{8}$$

which corresponds to the conservation of the total "mass" (or intensity) of the coupled system. The second one is

$$\int_{-\infty}^{\infty}\left(\psi_1\frac{\partial\bar{\psi}_1}{\partial t}+\psi_2\frac{\partial\bar{\psi}_2}{\partial t}\right)dt, \tag{9}$$

which corresponds, up to a constant, to the conservation of the total "momentum" of the system. The conserved integrals manifest themselves in the Hamiltonian formalism in the following conservation laws:

$$\rho_1+\rho_2=\text{const}, \tag{10}$$

$$\rho_1 p_1+\rho_2 p_2=\text{const}, \tag{11}$$

which relate to the first [Eq. (8)] and second [Eq. (9)] integrals, respectively.

It is then natural to transform to coordinates in which these conserved quantities are some of the new coordinates. We first transform canonically by the generating function

$$S_1\left(\varphi_1,\varphi_2,q_1,q_2,\tilde{\rho}_1,\tilde{\rho}_2,\tilde{p}_1,\tilde{p}_2\right)$$
$$=\left(\varphi_1-\varphi_2\right)\tilde{\rho}_1+\varphi_2\tilde{\rho}_2+\left(q_1+q_2\right)\tilde{p}_2+q_1\tilde{p}_1 \tag{12}$$

to the coordinates

$$\begin{aligned}
\tilde{\rho}_1&=\rho_1, & \tilde{\rho}_2&=\rho_1+\rho_2,\\
\tilde{\varphi}_1&=\varphi_1-\varphi_2, & \tilde{\varphi}_2&=\varphi_2,\\
\tilde{p}_1&=p_1-p_2, & \tilde{p}_2&=p_2,\\
\tilde{q}_1&=q_1, & \tilde{q}_2&=q_1+q_2,
\end{aligned} \tag{13}$$

in which the conserved quantity (10) is one of the momenta.

Next, we transform canonically by the generating function

$$S_2\left(\tilde{\rho}_1,\tilde{\rho}_2,\tilde{p}_1,\tilde{p}_2,\Phi_1,\Phi_2,Q_1,Q_2\right)$$
$$=-\left(\tilde{\rho}_1\tilde{p}_1+\tilde{\rho}_2\tilde{p}_2\right)Q_1-\tilde{p}_2Q_2-\tilde{\rho}_1\Phi_1-\tilde{\rho}_2\Phi_2 \tag{14}$$

to the coordinates

$$\begin{aligned}
R_1&=\tilde{\rho}_1, & R_2&=\tilde{\rho}_2,\\
\Phi_1&=\tilde{\varphi}_1-\frac{\tilde{p}_1\tilde{q}_1}{\tilde{\rho}_1}, & \Phi_2&=\tilde{\varphi}_2-\frac{\tilde{p}_2\tilde{q}_1}{\tilde{\rho}_1},\\
P_1&=\tilde{\rho}_1\tilde{p}_1+\tilde{\rho}_2\tilde{p}_2, & P_2&=\tilde{p}_2,\\
Q_1&=\frac{\tilde{q}_1}{\tilde{\rho}_1}, & Q_2&=\tilde{q}_2-\frac{\tilde{\rho}_2\tilde{q}_1}{\tilde{\rho}_1},
\end{aligned} \tag{15}$$

in which the conserved quantity (11) is one of the momenta. Note that the second transformation, Eq. (14), is singular for $R_1=0$. It can be shown that the "original" Hamiltonian, Eq. (6), does not have a fixed point at $R_1=0$. Therefore, in transforming to the new coordinates (15), we do not lose any essential information regarding the phase space structure of the system.

In the new coordinates the Hamiltonian is

$$H=H_0+H_{\text{int}}, \tag{16}$$

with

$$H_0=\frac{1}{4}\left[\frac{\left(P_1-R_2P_2\right)^2}{R_1}+R_2P_2^2+2P_2\left(P_1-R_2P_2\right)-\frac{1}{3}R_2^2-R_1^2R_2+R_2^2R_1\right], \tag{17a}$$

and

$$H_{\text{int}}=-\alpha\text{Re}\left[R_1\left(R_1-R_2\right)\exp\left(-i\Phi_1\right)\times\int_{-\infty}^{\infty}\frac{\exp\left[i\left(\frac{P_1-R_2P_2}{R_1}\right)t\right]}{\cosh\left(R_1t\right)\cosh\left[\left(R_2-R_1\right)t-Q_2\right]}dt\right]. \tag{17b}$$

We see that two of the momenta (R_2 and P_1) are indeed constants of motion. The equations of motion related to the Hamiltonian (17a) are too cumbersome. Therefore, we have written down the relevant (and nontrivial) equations of motion in the Appendix [see Eqs. (A1)– (A4)].

IV. FIXED POINTS ANALYSIS

We now look for the fixed points of the Hamiltonian system (17). We will be interested only in those fixed points, that correspond to the presence of a soliton in each of the two fibers. In doing so, we are ignoring the case when the soliton amplitude in one of the fibers is zero (this corresponds to either $\rho_1=0$ or $\rho_2=0$ or, in the new coordinates, to either $R_1=0$ or $R_1=R_2$). It would make no sense to employ our perturbation theory to these cases, since the evolution of optical pulses in the "unexcited" fiber would be better described (at least initially) by the linearized version of, say, Eq. (1b). Therefore, its solutions will not be in the form of solitons of the type of Eq. (2). Since we want to investigate soliton pulses when interacting in the NLDC, we shall also ignore those fixed points for which the soliton amplitude diminishes to zero as α tends to zero. As a matter of fact, we will be interested not in fixed points in the com-

plete parameter phase plane but those in a subspace of the phase plane. We shall call these steady-state points: points at which the evolution in the parameter space is such that the motion of the solitons will correspond to some steady (bound) state of the two-soliton (two-fiber-soliton) system.

Apart from the above-mentioned type of points, the steady-state points [see the Appendix, Eqs. (A5), (A7), (A9), and (A13)] are

$$\begin{aligned} &R_1 = \rho, \\ &R_2 = 2\rho, \\ &\Phi_1 = n\pi \quad (n = 0, 1), \\ &Q_1 = 0, \\ &\frac{P_1 - P_2 R_2}{R_1} = 0. \end{aligned} \tag{18}$$

Transforming back [using Eqs. (13) and (15)] to our "laboratory" coordinates, Eqs. (18) read as

$$\begin{aligned} &\rho_1 = \rho_2 \equiv \rho, \\ &\varphi_1 - \varphi_2 = n\pi \quad (n = 0, 1), \\ &p_1 = p_2 \equiv p, \\ &q_1 - q_2 = 0. \end{aligned} \tag{19}$$

These steady-state points correspond to two identical, that is, having the same amplitude ρ and the same velocity p, solitons. They also have the same center of mass, i.e., they are peaked around the same coordinate as they evolve in the NLDC. The only difference between the n=0 and n=1 points is the relative phase of the solitons (0 and π, respectively). Notice that some (those for which $p = 0$) of these soliton states have been used [7,18] as starting points for perturbation theory analysis.

V. LINEAR STABILITY ANALYSIS

Having obtained the steady-state points of the system, we now turn to investigate their linear stability. We look at parameter values that are close to the steady-state ones, that is,

$$\begin{aligned} &R_1(x) = \rho + r_1(x), \\ &R_2(x) = 2\rho + r_2(x), \\ &\Phi_1(x) = n\pi + \beta_n(x), \\ &P_1(x) = 2\rho p + \delta_1(x), \\ &P_2(x) = p + \delta_2(x), \\ &Q_2(x) = \mu(x). \end{aligned} \tag{20}$$

Note that in the Hamiltonian formalism we are able to look at the variation of *all* the parameters of the solitons, while preserving the (Hamiltonian) structure of the full [Eqs. (1)] system. This is not the case when using [7,18,19] other types of perturbation analysis, which limit the variations allowed in the values of the parameters. Also, the functional form of the variation of the parameters is obtained from our theory, self-consistently, and is not put in "by hand," as in the Lagrangian formulation [7,19].

Inserting these into Eqs. (A1)–(A4) and linearizing, we obtain the following set of linearized equations:

$$r_1' = \alpha\rho(1)^{n+1}\beta_n, \tag{21a}$$

$$r_2' = 0, \tag{21b}$$

$$\beta_n' = -\left[\rho + \frac{\alpha(-1)^{n+1}}{\rho}\left(\frac{\pi^2}{18} + \frac{2}{3}\right)\right](2r_1 - r_2), \tag{21c}$$

$$\delta_1' = 0, \tag{21d}$$

$$\delta_2' = \frac{\alpha(-1)^{n+1}\rho}{3}\mu, \tag{21e}$$

$$\mu' = -\left[1 - \frac{\alpha(-1)^{n+1}}{\rho^2}\frac{\pi^2}{3}\right](\delta_1 - 2\rho\delta_2 - pr_2), \tag{21f}$$

where we have obtained Eqs. (21b) and (21d) by using the fact that R_2 and P_1 are conserved quantities of the system (17) [see Eqs. (10) and (11)]. The prime denotes the "time" derivative (that is, $\partial/\partial x$). A similar analysis was carried out in [20], but the deviations (from the steady-state values) of the amplitudes and their phases [that is, Eqs. (21a) and (21c)] were ignored there.

We differentiate Eqs. (21a) and (21e) once again. Using Eqs. (21b)–(21f), we obtain two second-order equations

$$(2r_1 - r_2)'' = -\omega_1^2(2r_1 - r_2) \tag{22}$$

and

$$\delta_2'' = -\omega_2^2\delta_2 + \frac{\omega_2^2}{2\rho}(\delta_1 - pr_2), \tag{23}$$

where

$$\omega_1^2 = (-1)^{n+1}2\alpha\rho^2\left[1 + \frac{\alpha(-1)^{n+1}}{\rho^2}\left(\frac{\pi^2}{18} + \frac{2}{3}\right)\right] \tag{24}$$

and

$$\omega_2^2 = (-1)^n\frac{2}{3}\alpha\rho^2\left[1 - \frac{\alpha(-1)^{n+1}}{\rho^2}\left(\frac{\pi^2}{3}\right)\right]. \tag{25}$$

From Eqs. (24) and (25) we see that, for n=1, ω_1 is always positive while ω_2 is negative provided $\alpha \ll \rho^2$, which holds in our case since we are assuming that $\rho \gg \alpha$ and $\rho \gtrsim 1$. For the n=0 steady-state points the situation is the opposite: ω_2 is always positive, while ω_1 is negative for $\alpha \ll \rho^2$. Thus we conclude that the system (17), in general, has no stable steady-state points. For each of the two types of steady-state points there exist stable and unstable manifolds (types of perturbations). For the n=0 points, perturbations of the type $r_1(x) \neq 0$ are unstable, while those of the type $\delta_2(x) \neq 0$ [or $\mu(x) \neq 0$] are stable. For the n=1 type of points the situation is the opposite. As mentioned above, a result similar to Eq. (23) was obtained in [20]. However, since Eq. (22) was not obtained there, this led to the wrong prediction that

the system (1) does possess stable bound states. In [21] the linear stability analysis yielded (qualitatively) different results. In [19] the result (23) was obtained; however, the use of the Lagrangian formalism did not make it possible to find the oscillations (or the divergence) in the values of the amplitudes of the solitons.

VI. NUMERICAL SIMULATIONS

In order to check the validity of the theoretical analysis presented in Secs. III–V, we performed numerical simulations with Eqs. (1). The simulations were done using a modified version of the well-known split-step Fourier transform method [25], with periodic boundary conditions. The initial conditions were in the form of the single-soliton solutions [Eq. (2)] of the unperturbed system, with parameter values close to the steady-state point ones. That is, we chose

$$\psi_1(0,t) = -i\frac{\frac{\rho}{2}\exp(ipt)}{\cosh\left(\frac{\rho t}{2}\right)},$$
$$\psi_2(0,t) = -i\frac{\frac{(\rho-\delta\rho)}{2}\exp\left[i\left(pt+n\pi\right)\right]}{\cosh\left(\frac{(\rho-\delta\rho)t}{2}+\delta q\right)}, \qquad (26)$$

with n=0 or 1. $\delta\rho$ and δq are the deviations from the steady-state point values.

In Fig. 1 we show contour plots of the intensities $|\psi_1(x,t)|^2$ and $|\psi_2(x,t)|^2$ for a stable perturbation of the type $\delta\rho \neq 0$, $\delta q = 0$, and n=1. The steady oscillations in the amplitudes (maximum values) of each of the solitons are clearly seen. Figure 2 shows the contour plots for the second type of stable perturbations, those of the type $\delta\rho = 0$, $\delta q \neq 0$, and n=0. Here the centers of masses of the solitons oscillate, while their maxima remain constant. In Fig. 3 a perturbation of the type $\delta\rho = 0$, $\delta q \neq 0$, and n=1 was chosen and the instability is clearly seen. Note that after the instability separates the solitons a distance farther than their typical widths, they do not interact anymore and their motion is that of the unperturbed [see Eq. (2)] solitons, with the values of p_1 and p_2 reached by the "time" the interaction ceased.

We checked numerically the predictions of Eqs. (24) and (25) for the frequency of oscillations in the values of the parameters of the solitons under the two types of stable perturbations. Figure 4 shows the comparison between the theoretical prediction, obtained from Eq. (24), and the values computed numerically, of the dependence of the frequency ω_1 on the coupling parameter α for the case of perturbations of the type $\delta\rho \neq 0$, $\delta q = 0$, and n=1. A typical value of $\rho = 4$ was chosen. It is seen that the correspondence between the numerical results

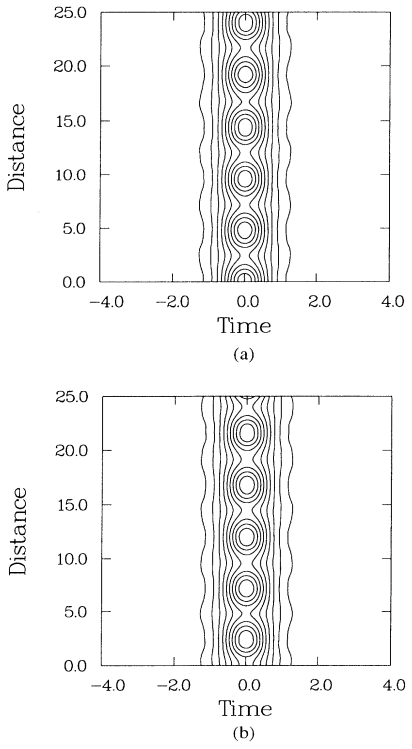

FIG. 1. Contour plot of the normalized intensities (a) $|\psi_1(x,t)|^2$ and (b) $|\psi_2(x,t)|^2$ as a function of dimensionless time t and scaled propagation distance x. The initial pulse profiles are in the form of Eq. (26) with $\rho = 4$, $p = 0$, and $n = 1$. $\delta\rho = 0.8$, $\delta q = 0$, and $\alpha = 0.075$. As can be seen, this is indeed a stable perturbed state of the two-soliton system.

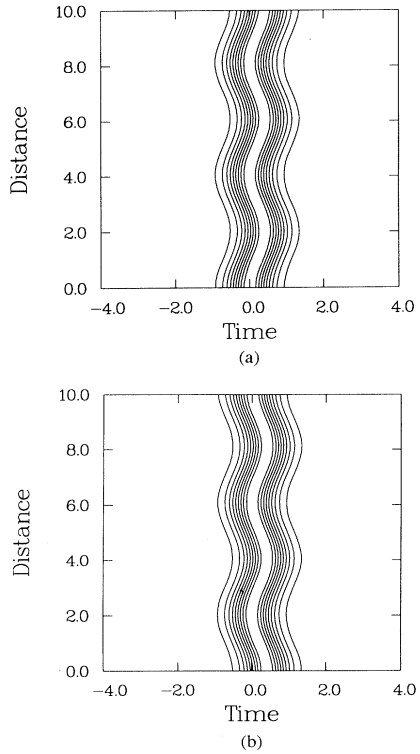

FIG. 2. Contour plot of the intensities (a) $|\psi_1(x,t)|^2$ and (b) $|\psi_2(x,t)|^2$. The initial pulse profiles are in the form of Eq. (26) with $\rho = 5$, $p = 0$, and $n = 1$. $\delta\rho = 0$, $\delta q = 0.8$, and $\alpha = 0.2$. This, again, is a stable perturbed state.

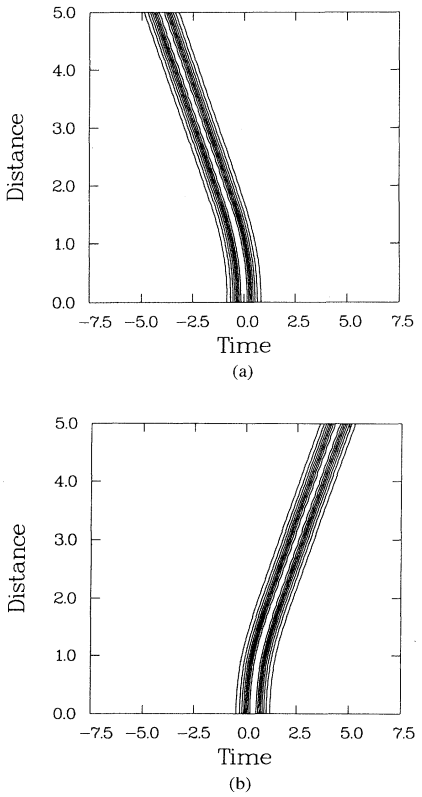

FIG. 3. Contour plot of the intensities (a) $|\psi_1(x,t)|^2$ and (b) $|\psi_2(x,t)|^2$. The initial pulse profiles are in the form of Eq. (26) with $\rho = 5$, $p = 0$, and $n = 1$. $\delta\rho = 0$, $\delta q = 0.8$, and $\alpha = 0.2$. After the exponential divergence separates the solitons more than their widths $(1/\rho)$ apart, they do *not* interact any more and the motion of their center of masses is uniform, like that of the unperturbed [Eq. (2)] solitons.

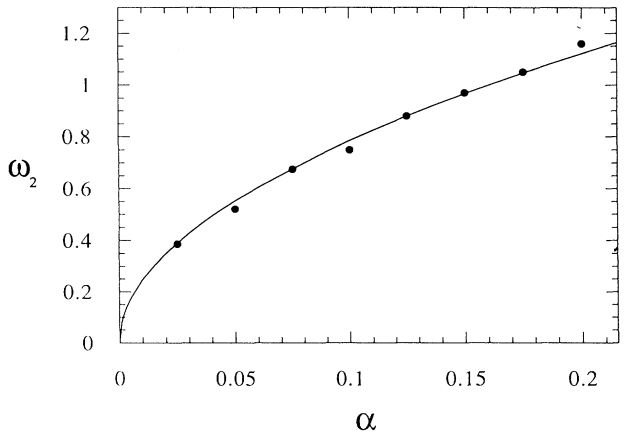

FIG. 5. Frequency of oscillations in the coordinates of the center of mass (c.m.) of the solitons as a function of α, in the case of stable perturbations of the type $\delta\rho = 0$, $\delta q \neq 0$, and n=0, for a typical value of $\rho = 3$. The line corresponds to the theoretical prediction [see Eq. (25)] and the dots are the values obtained from the numerical simulations.

and the theoretical prediction is very good. In Fig. 5 the numerical and theoretical [obtained from Eq. (25)] results are compared for the dependence of the frequency ω_2 on α for the case of perturbations of the type $\delta\rho = 0$, $\delta q \neq 0$, and n=0. A typical value of $\rho = 3$ was chosen. Here, again, the numerical results agree well with the theoretical predictions.

The behavior of the two-soliton system under unstable perturbations was also studied numerically. In Fig. 6 the difference between the amplitudes of the two solitons is plotted as a function of the distance of propagation for an unstable perturbation of the type $\delta\rho \neq 0$, $\delta q = 0$, and n=0. We chose $\rho = 4$ and $\alpha = 0.075$. The line represents the solution of the linearized equations Eq. (22) with the

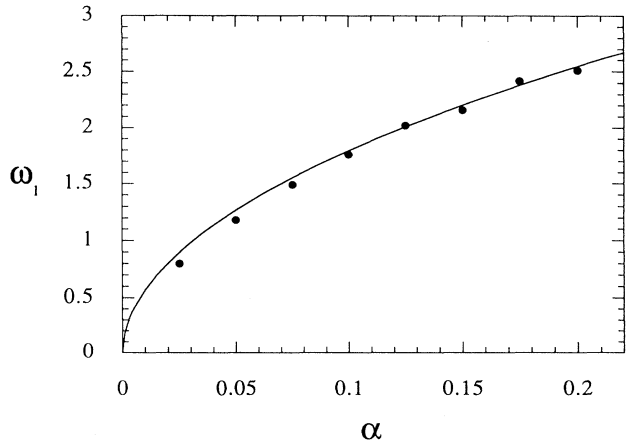

FIG. 4. Frequency of oscillations in the amplitudes of the solitons as a function of α. The initial conditions are in the form of stable perturbations of the type $\delta\rho \neq 0$, $\delta q = 0$, and n=1, for a representative value of $\rho = 4$. The line corresponds to the theoretical prediction [see Eq. (24)] and the dots are the values obtained from the numerical simulations.

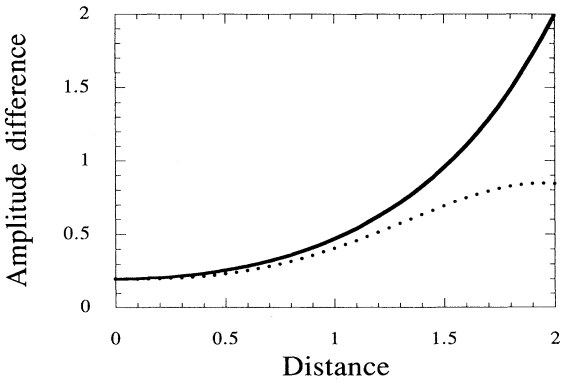

FIG. 6. Difference between the amplitudes of the two solitons as a function of distance x for unstable perturbations of the type $\delta\rho \neq 0$, $\delta q = 0$ and n=0. $\rho = 4$ and $\alpha = 0.075$. The line corresponds to $\delta\rho\cosh(\omega_1 t)$, which is the theoretical prediction. ω_1 was obtained from the simulations in the n=1 case, when these type of perturbations are stable. The dots are the values obtained from the numerical simulations.

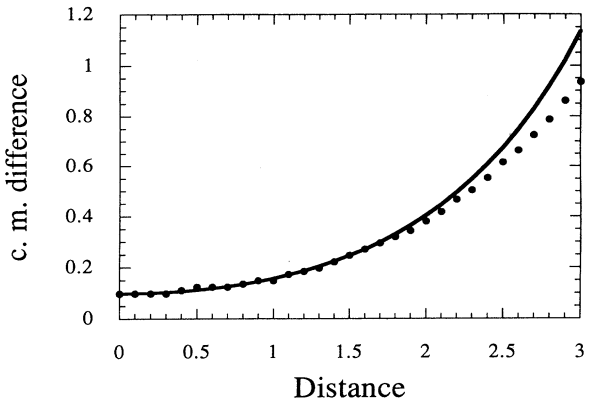

FIG. 7. Difference between the c.m. of the two solitons as a function of distance x for unstable perturbations of the type $\delta\rho = 0$, $\delta q \neq 0$, and n=1. $\rho = 4$ and $\alpha = 0.1$. The line corresponds to $\delta q \cosh(\omega_2 t)$, which is the theoretical prediction. ω_2 was obtained from the simulations in the n=0 case, when these type of perturbations are stable. The dots are the values obtained from the numerical simulations.

value of ω_1 taken from the corresponding numerical simulations when this type of perturbation is stable (i.e., n=1). The dots represent the values obtained numerically. It can be seen from the figure that the exponential deviation saturates rather quickly. (The exponent has the value of 0.9 when the discrepancy between the theoretical and numerical results reaches 10%.) On the other hand, in the case of unstable perturbations of the type $\delta\rho = 0$, $\delta q \neq 0$, and n=1, shown in Fig. 7, there is quite good agreement (the discrepancy between the theoretical and numerical results is less than 10% when the exponent reaches a value of 2.7) between the theoretical predictions, obtained from Eq. (23), and the numerical results. In this case the exponential deviation also ceases (as seen in Fig. 3) when the two solitons are far enough apart.

VII. SUMMARY

We have studied analytically and numerically the interaction of soliton pulses in the nonlinear directional fiber coupler (NLDC). Our aim was to look for bound soliton states and investigate their stability. Exploiting the Hamiltonian structure of the evolution equations, we developed a canonical perturbation theory for the evolution of the parameters of two solitons, interacting in the NLDC. Within the framework of the perturbation theory, all the conserved integrals of the exact problem were preserved

Exactly two families of bound two-soliton states were found and their stability analysis showed that, in general, neither of these states is stable. For each of the states there exist stable and unstable types of perturbations. The linear stability analysis was performed without any restrictions on the evolution of the parameters of the solitons, leading to complete results as to the stability of these bound states.

The numerical simulations that we performed confirmed the existence of two types of stable perturbations. The numerical results agreed quantitatively with the theoretical predictions for the frequency of small oscillations. The two types of unstable perturbations were also observed numerically. There is good agreement between the values of the instability growth rates obtained theoretically and numerically. In the case of the unstable perturbations of the type $\delta q \neq 0$ (n=1) the linear approximation obviously breaks down when the two solitons are sufficiently far apart (because they do not interact any more), as was indeed observed numerically. For unstable perturbations of the type $\delta\rho \neq 0$ (n=0) it is not clear when the linear approximation does not hold anymore. Numerically, we observed a saturation of the exponential divergence after a relatively short (the exponent reached a value of 0.9) distance. This subject is currently under further investigation.

ACKNOWLEDGMENTS

We are extremely grateful to B. Meerson for continuous interest and advice and for a critical reading of the manuscript.

APPENDIX

In this appendix we shall show the detailed derivation of the evaluation of the steady-state points of the Hamiltonian (17). The relevant (and nontrivial) equations of motion corresponding to the Hamiltonian (17) are

$$R_1' = -\frac{\partial H_{\rm int}}{\partial \Phi_1} = \alpha {\rm Im}\left[R_1 (R_1 - R_2)\exp(-i\Phi_1)\int_{-\infty}^{\infty} \frac{\exp\left[i\left(\frac{P_1 - R_2 P_2}{R_1}\right)t\right]}{\cosh(R_1 t)\cosh[(R_2 - R_1)t - Q_2]}dt\right], \tag{A1}$$

$$P_2' = -\frac{\partial H_{\rm int}}{\partial Q_2} = \alpha {\rm Re}\left[R_1 (R_1 - R_2)\exp(-i\Phi_1)\int_{-\infty}^{\infty} \frac{\exp\left[i\left(\frac{P_1 - R_2 P_2}{R_1}\right)t\right]\sinh[(R_2 - R_1)t - Q_2]}{\cosh(R_1 t)\cosh^2[(R_2 - R_1)t - Q_2]}dt\right], \tag{A2}$$

$$\Phi_1' = \frac{\partial H}{\partial R_1} = -\frac{(P_1 - R_2P_2)^2}{2R_1^2} - \left(R_1R_2 - \frac{R_2^2}{2}\right)$$
$$+\alpha \mathrm{Re}\Bigg(R_1(R_1 - R_2)\exp(-i\Phi_1)\Bigg\{\int_{-\infty}^{\infty} \frac{\exp\left[i\left(\frac{P_1 - R_2P_2}{R_1}\right)t\right]}{\cosh(R_1t)\cosh[(R_2 - R_1)t - Q_2]}\left(\frac{1}{R_2 - R_1} - \frac{1}{R_1}\right)dt$$
$$+\int_{-\infty}^{\infty} \frac{\exp\left[i\left(\frac{P_1 - R_2P_2}{R_1}\right)t\right]t}{\cosh(R_1t)\cosh[(R_2 - R_1)t - Q_2]}\left[i\left(\frac{P_1 - R_2P_2}{R_1^2}\right) + \tanh(R_1t)\right.$$
$$\left. - \tanh[(R_2 - R_1)t - Q_2]\right]dt\Bigg\}\Bigg), \tag{A3}$$

$$Q_2' = \frac{\partial H}{\partial P_2} = (P_1 - R_2P_2)\left(1 - \frac{R_2}{R_1}\right) - \alpha \mathrm{Im}\left[R_2(R_1 - R_2)\exp(-i\Phi_1)\int_{-\infty}^{\infty} \frac{\exp\left[i\left(\frac{P_1 - R_2P_2}{R_1}\right)t\right]t}{\cosh(R_1t)\cosh[(R_2 - R_1)t - Q_2]}dt\right]. \tag{A4}$$

It can be shown that no steady-state points exist for which $\rho_1 \neq \rho_2$. In the new coordinates [see Eqs. (13) and (15)], this translates to

$$R_1 = \rho_1 \equiv \rho, \quad R_2 = \rho_1 + \rho_2 \equiv 2\rho. \tag{A5}$$

For these values of R_1 and R_2 the integral in Eq. (17b) can be evaluated by integration in the complex plain. For $Q_2 \neq 0$ and $(P_1 - R_2P_2) \neq 0$, we obtain

$$H_{\mathrm{int}} = -\alpha\rho\pi \mathrm{Im}\left[\frac{\exp\left\{i\left[\frac{(P_1 - 2\rho P_2)}{\rho^2}Q_2 - \Phi_1\right]\right\}}{\sinh\left[\pi\left(\frac{P_1 - 2\rho P_2}{2\rho^2}\right)\right]\sinh(Q_2)}\right]. \tag{A6}$$

It can be seen that, in Eq. (A6), $R_1' = \partial H_{\mathrm{int}}/\partial\Phi_1$ and $P_2' = \partial H_{\mathrm{int}}/\partial Q_2$ cannot be set equal to zero simultaneously. Thus there are no steady-state points at which $Q_2 \neq 0$ and $(P_1 - R_2P_2) \neq 0$, so that either Q_2 or $(P_1 - R_2P_2)$ must be 0. Setting

$$Q_2 = 0, \tag{A7}$$

we integrate Eq. (17b) and obtain

$$H_{\mathrm{int}} = -\alpha\rho\pi \mathrm{Re}\left[\frac{\left(\frac{P_1 - 2\rho P_2}{2\rho^2}\right)\exp(-i\Phi_1)}{\sinh\left[\pi\left(\frac{P_1 - 2\rho P_2}{2\rho^2}\right)\right]}\right]. \tag{A8}$$

Equating, from (A8), $R_1' = \partial H_{\mathrm{int}}/\partial\Phi_1$ to 0, we obtain the condition

$$\Phi_1 = n\pi, \quad n = 0, 1. \tag{A9}$$

Using the condition (A9), we obtain from Eq. (A2)

$$P_2' = \left.\frac{\partial H_{\mathrm{int}}}{\partial Q_2}\right|_{Q_2=0} = 0, \tag{A10}$$

so that both momenta R_1 and P_2 are constant at these points [Eqs. (A5), (A7), and (A9)]. In order that these points correspond to steady-state points we also require that Eqs. (A7) and (A9) hold. That is, Φ_1' and Q_2' must be equal to 0. Inserting all the relations into Eqs. (A3) and (A4), we obtain

$$Q_2' = \frac{\partial H}{\partial P_2}$$
$$= -(P_1 - 2\rho P_2) - 2\alpha \mathrm{Im}\left[(-1)^n \times \int_{-\infty}^{\infty} \frac{\exp\left[i\left(\frac{P_1 - 2\rho P_2}{\rho^2}\right)t\right]t}{\cosh^2(t)}dt\right] \tag{A11}$$

and

$$\Phi_1' = \frac{\partial H}{\partial R_1} = -\frac{(P_1 - 2\rho P_2)^2}{2\rho^2}$$
$$-\alpha \mathrm{Im}\left[(-1)^n\left(\frac{P_1 - 2\rho P_2}{\rho^2}\right) \times \int_{-\infty}^{\infty} \frac{\exp\left[i\left(\frac{P_1 - 2\rho P_2}{\rho^2}\right)t\right]t}{\cosh^2(t)}dt\right]. \tag{A12}$$

It can be seen that Eqs. (A11) and (A12) can be set to equal 0 if and only if $(P_1 - 2\rho P_2) = 0$. Remembering that 2ρ is R_2 at the sought for steady-state points gives us the final constraint for the existence of steady-state points:

$$(P_1 - R_2P_2) = 0. \tag{A13}$$

Note that if instead of first setting Q_2 to equal 0 we first set $(P_1 - R_2P_2)$ to equal 0, we still get the same relations for the steady-state points.

[1] G. P. Agrawal, *Nonlinear Fiber Optics* (Academic, Boston, 1989).
[2] L. F. Mollenauer, E. Lichtman, M. J. Neubelt, and G. T. Harvey, in *Proceedings of the Conference on Optical Fiber Communications* (Optical Society of America, Washington, DC, 1993); M. Nakazawa, K. Suzuki, E. Yamada, H. Kubota, Y. Kimura, and M. Takaya, *ibid.*
[3] A. A. Maier, Kvant. Elektron. (Moscow) **9**, 2296 (1982) [Sov. J. Quantum Electron. **12**, 1490 (1982)].
[4] S. M. Jensen, IEEE J. Quantum Electron. **QE-18**, 1580 (1982).
[5] D. D. Gusovskii, E. M. Dianov, A. A. Maier, V. B. Neustruev, E. I. Shklovskii, and A. Shcherbakov, Kvant. Ekeltron. (Moscow) **12**, 2312 (1985) [Sov. J. Quantum Electron. **15**, 1523 (1985)].
[6] S. R. Friberg, Y. Silberberg, M. K. Oliver, M. J. Andrejco, M. A. Saifik, and P. W. Smith, Appl. Phys. Lett. **51**, 1135 (1987).
[7] C. Paré and M. Florjańczyk, Phys. Rev. A **41**, 6287 (1990).
[8] I. M. Uzunov, R. Muschall, M. Gölles, Yu. S. Kivshar, B. A. Malomed, and F. Lederer, Phys. Rev. E **51**, 2527 (1995).
[9] S. Trillo, S. Wabnitz, E. M. Wright, and G. I. Stegeman, Opt. Lett. **13**, 672 (1988).
[10] E. Caglioti, S. Trillo, S. Wabnitz, B. Crosignani, and P. Di Porto, J. Opt. Soc. Am. B **7**, 374 (1990).
[11] D. Anderson, Phys. Rev. A **27**, 3135 (1983).
[12] A. Hasegawa and F. Tappert, Appl. Phys. Lett. **23**, 142 (1973).
[13] S. P. Novikov, S. V. Manakov, L. P. Pitaevsky, and V. E. Zakharov, *Theory of Solitons. The Inverse Scattering Method* (Consultants Bureau, New York, 1984).
[14] V. E. Zakharov and E. I. Schulman, Physica D **4**, 270 (1982).
[15] N. Akhmediev and A. Ankiewicz, Phys. Rev. Lett. **70**, 2395 (1993).
[16] J. M. Soto-Crespo and N. Akhmediev, Phys. Rev. E **48**, 4710 (1993).
[17] N. Akhmediev and J. M. Soto-Crespo, Phys. Rev. E **49**, 4519 (1994).
[18] E. M. Wright, G. I. Stegeman, and S. Wabnitz, Phys. Rev. A **40**, 4455 (1989).
[19] S. L. Doty, J. W. Haus, YunJe Oh, and R. L. Fork, Phys. Rev. E **51**, 709 (1995).
[20] F. Kh. Abdullaev, R. M. Abrarov, and S. A. Darmanyan, Opt. Lett. **14**, 131 (1989).
[21] Y. S. Kivshar and B. A. Malomed, Opt. Lett. **14**, 1365 (1989).
[22] L. F. Mollenauer, R. H. Stolen, and J. P. Gordon, Phys. Rev. Lett. **45**, 1095 (1980).
[23] A. W. Snyder and J. D. Love, *Optical Waveguide Theory* (Chapman and Hall, London, 1983).
[24] L. D. Faddeev and L. A. Takhtajan, *Hamiltonian Methods in the Theory of Solitons* (Springer-Verlag, Berlin, 1987).
[25] R. H. Hardin and F. D. Tappert, SIAM Rev. Chron. **15**, 423 (1973).